

First principles prediction of a morphotropic phase boundary in the $\text{Bi}(\text{Zn}_{1/2}\text{Ti}_{1/2})\text{O}_3 - (\text{Bi}_{1/2}\text{Sr}_{1/2})(\text{Zn}_{1/2}\text{Nb}_{1/2})\text{O}_3$ alloy

Valentino R. Cooper, Asegun S. Henry, Shigeyuki Takagi, and David J. Singh

Citation: *Applied Physics Letters* **98**, 122903 (2011); doi: 10.1063/1.3570626

View online: <http://dx.doi.org/10.1063/1.3570626>

View Table of Contents: <http://scitation.aip.org/content/aip/journal/apl/98/12?ver=pdfcov>

Published by the [AIP Publishing](#)

Articles you may be interested in

Anisotropy of ferroelectric behavior of $(1-x)\text{Bi}_{1/2}\text{Na}_{1/2}\text{TiO}_3-x\text{BaTiO}_3$ single crystals across the morphotropic phase boundary

J. Appl. Phys. **116**, 044111 (2014); 10.1063/1.4891529

Role of coexisting tetragonal regions in the rhombohedral phase of $\text{Na}_{0.5}\text{Bi}_{0.5}\text{TiO}_3-x\text{at.}\% \text{BaTiO}_3$ crystals on enhanced piezoelectric properties on approaching the morphotropic phase boundary

Appl. Phys. Lett. **100**, 012901 (2012); 10.1063/1.3673832

First-principles prediction of a two dimensional electron gas at the $\text{BiFeO}_3/\text{SrTiO}_3$ interface

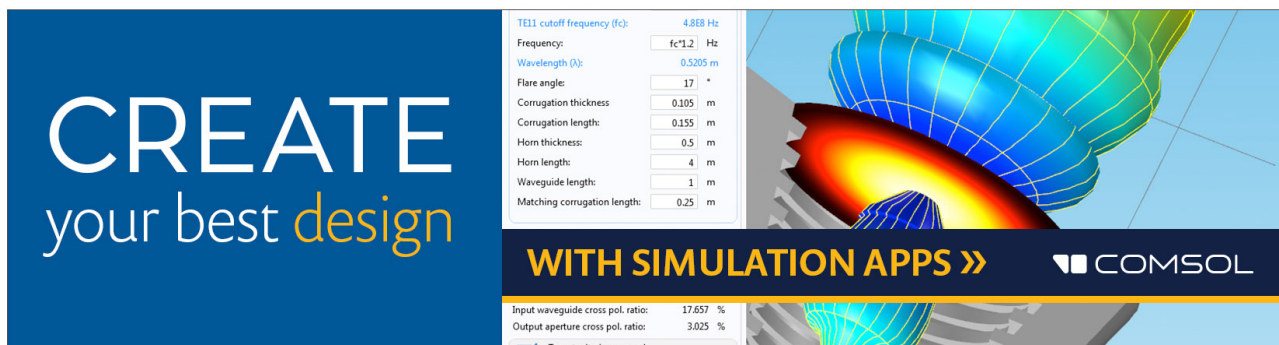
Appl. Phys. Lett. **99**, 062902 (2011); 10.1063/1.3624457

Systematic ab initio study of the phase diagram of epitaxially strained SrTiO_3

J. Appl. Phys. **100**, 084104 (2006); 10.1063/1.2358305

Predicting morphotropic phase boundary locations and transition temperatures in Pb- and Bi-based perovskite solid solutions from crystal chemical data and first-principles calculations

J. Appl. Phys. **98**, 094111 (2005); 10.1063/1.2128049



CREATE
your best design

TE11 cutoff frequency (fc): 4.868 Hz
Frequency: Hz
Wavelength (lambda): 0.5205 m
Flare angle: °
Corrugation thickness: m
Corrugation length: m
Horn thickness: m
Horn length: m
Waveguide length: m
Matching corrugation length: m

WITH SIMULATION APPS » 

Input waveguide cross pol. ratio: 17.657 %
Output aperture cross pol. ratio: 3.025 %
 Target criterion: passed

First principles prediction of a morphotropic phase boundary in the $\text{Bi}(\text{Zn}_{1/2}\text{Ti}_{1/2})\text{O}_3 - (\text{Bi}_{1/2}\text{Sr}_{1/2})(\text{Zn}_{1/2}\text{Nb}_{1/2})\text{O}_3$ alloy

Valentino R. Cooper,^{1,a)} Asegun S. Henry,^{2,3} Shigeyuki Takagi,^{1,2} and David J. Singh¹

¹Materials Science and Technology Division, Oak Ridge National Laboratory, Oak Ridge, Tennessee 37831, USA

²Department of Physics, University of Tennessee, Knoxville, Tennessee 37996, USA

³George W. Woodruff School of Mechanical Engineering, Georgia Institute of Technology, Atlanta 30332, Georgia

(Received 8 November 2010; accepted 2 March 2011; published online 22 March 2011)

The magnitude and direction of polarization within alloys of the tetragonally distorted $\text{Bi}(\text{Zn}_{1/2}\text{Ti}_{1/2})\text{O}_3$ (BZT) and the rhombohedrally oriented $(\text{Bi}_{1/2}\text{Sr}_{1/2})(\text{Zn}_{1/2}\text{Nb}_{1/2})\text{O}_3$ are explored using density functional theory. For compositions with $\geq 50\%$ of BZT, we find that the polarization is mainly in the [001] direction. Conversely, for low concentrations of BZT the polarization is rhombohedrally oriented. Based on these results we propose a phase diagram with a monoclinic phase that appears when the BZT concentration is roughly 50%. At this concentration, the material may have a useful piezoelectric response. © 2011 American Institute of Physics.

[doi:10.1063/1.3570626]

Due to the toxicity of lead, the discovery of Pb free piezoelectrics has been the subject of much research over the past few decades. One strategy for maximizing electromechanical responses has been to alloy tetragonal and rhombohedral ferroelectrics. The combination of two such compounds often results in a compositionally dependent region, the morphotropic phase boundary (MPB), where the crystal structure abruptly undergoes a transition between the macroscopic phases of the parent compounds.¹ A prototypical example is the solid-solution of the tetragonally distorted PbTiO_3 (PT) and the antiferrodistorted PbZrO_3 (PZ). This transformation, which is mediated by a monoclinic phase, occurs in a narrow compositional range (of only a few percent) near 50%PT–50%PZ.² In general, ferroelectric alloys near MPBs exhibit enhanced electromechanical responses when the parent compounds have high remnant polarizations, \vec{P} .³

Currently, many of the best piezoelectric materials available have significant amounts of Pb due to preferential alloying with the strongly tetragonal PT.⁴ An alternative exists in Bi-based ferroelectrics. Similar to Pb, Bi has stereochemically active lone pairs and a small ionic radius. This combination results in compounds with relatively large A-site cation displacements and Born effective charges in a small volume, producing high \vec{P} .⁵ Unfortunately, the majority of Bi containing compounds are either rhombohedrally distorted or inferior to PT. For example, in a previous study we predicted that the double perovskite $(\text{Bi}_{1/2}\text{Sr}_{1/2})(\text{Zn}_{1/2}\text{Nb}_{1/2})\text{O}_3$ (BSZN) has a pseudocubic structure with a relatively high remnant polarization ($\sim 79 \mu\text{C}/\text{cm}^2$) pointing along [111].⁶ However, there is recent experimental evidence for supertetragonal Bi ferroelectrics, such as appropriately strained BiFeO_3 .⁷ Also, significantly enhanced tetragonality was observed when PbTiO_3 was alloyed with $\text{BiZn}_{1/2}\text{Ti}_{1/2}\text{O}_3$ (BZT).⁸ Subsequent experiments and first-principles calculations demonstrated that BZT indeed has a substantially large c/a with \vec{P}

greater than that of PT by 50%, making it a good candidate for a tetragonal end member for piezoelectrics.^{9,10} However, the supertetragonality of these materials limits their usefulness as ferroelectrics as they require strong electric fields to switch the polarization.

In this letter, we use first principles density functional theory (DFT) to study the polar behavior as a function of composition of the BZT–BSZN compound. We examine the magnitude and orientation of the polarization as a function of BZT concentration. Our results yield mostly tetragonal distortions for BZT concentrations $\geq 50\%$ and a rotation of the polarization to a [111] orientation for concentrations $\leq 25\%$. More importantly, this points to the presence of a monoclinic phase with 50% BZT concentration. Due to the significant differences in the structural parameters between the tetragonal and the rhombohedral phases, this region may have high piezoresponses.

We perform DFT supercell calculations for alloys of BZT–BSZN using the local density approximation for exchange and correlation and ultrasoft pseudopotentials¹¹ as implemented in the QUANTUM ESPRESSO simulation package (v. 4.1.2).¹² A 50 Ry cutoff and a $4 \times 4 \times l$ k -point mesh were used, where $l=4$ for $2 \times 2 \times 2$ (40 atoms) supercells and $l=2$ for $2 \times 2 \times 4$ (80 atoms) supercells. 40 atom supercells were modeled for the end member calculations, while two 80 atom supercells were studied for each of the 50%–50% and 25%–75% BZT–BSZN mixtures. (Since similar lattice constants were obtained for these configurations, we report only on the lowest energy configuration.) The charge difference between Zn^{2+} and $\text{Nb}^{5+}/\text{Ti}^{4+}$ is expected to lead to a strong ordering tendency on the B-site.^{13–15} Hence B-cations were arranged such that the Zn and Nb/Ti were on separate rocksalt-ordered sublattices placing excess cations on the deficient site. Note, there is also a considerable size difference between the radius of Zn ($r_{\text{Zn}}=0.74 \text{ \AA}$) and Nb/Ti ($r_{\text{Ti}}=0.605 \text{ \AA}$, $r_{\text{Nb}}=0.64 \text{ \AA}$). Although no ordering preference is expected for A-site cations, rocksalt-type orderings were simulated for Bi and Sr to reduce any symmetry related bias (see insets of Fig. 1 and Ref. 16). In all cases, the unit cells

^{a)}Electronic mail: coopervr@ornl.gov.

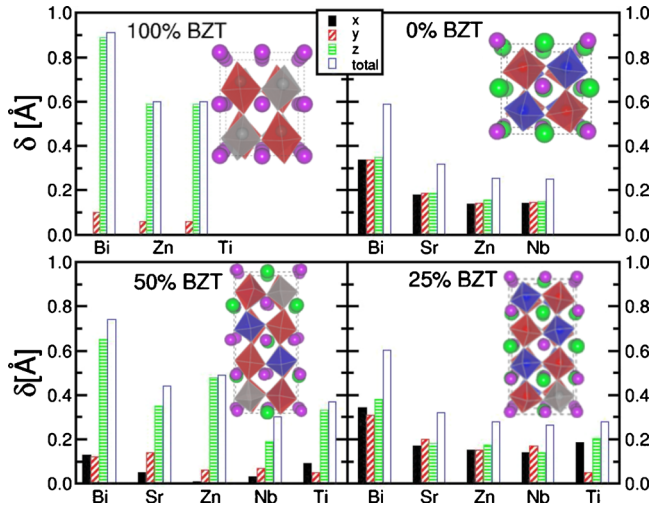


FIG. 1. (Color online) Average off-centering, δ , for each cation in the four BZT-BSZN compositions studied. Solid, diagonal stripes, horizontal stripes, and empty bars represent x , y , z , and total displacements, respectively. Insets show cation arrangements. Ions and corresponding octahedra are colored (online only) as follows; Bi: magenta, Sr: green, Zn: red, Ti: gray, and Nb: blue. Also see Ref. 16 for alloy cation orderings.

were chosen to minimize any symmetry bias. By using 80 atom unit cells we were able to study a sufficient number of local configurations in order to properly describe the microstructure of the alloy materials. All ionic coordinates were fully relaxed until the Hellman–Feynman forces on the ions were less than 7 meV/Å. All polarization calculations were performed using the Berry phase method.¹⁷

For rocksalt-ordered BZT, our calculated tetragonal lattice constants of $a=3.74$ Å, $c=4.58$ Å give a $c/a=1.22$, which is consistent with previous DFT calculations. It should be noted that a number of different B -cation arrangements were previously explored for the BZT structure, all giving similar values for c/a and polarization.¹⁰ Our computed polarization of $142 \mu\text{C}/\text{cm}^2$ points along the $[001]$ direction and is in excellent agreement with recent DFT predictions and the experiment.^{9,10} As we previously demonstrated, the BSZN end member has $a=3.95$ Å with $\vec{P}=77 \mu\text{C}/\text{cm}^2$ aligned along $[111]$.⁶

To explore the effect of alloying, we first examine the 50% BZT–50% BSZN composition. As was the case with pure BZT compound, we find that the 50%–50% alloy has an unusually high polarization of $114 \mu\text{C}/\text{cm}^2$. The fact that the polarization points 14° away from the $[001]$ direction and gives rise to monoclinic distortions (with $c/a=1.11$; see Table I), suggests that a MPB may indeed exist near concentrations of 50% BZT. For comparison, we studied the 25% BZT–75% BSZN alloy. For the arrangement studied we

found lattice constants that are nearly identical to the pure BSZN compound (Table I). Likewise, the polarization of $81 \mu\text{C}/\text{cm}^2$ points along the $[111]$ direction.

To understand the microscopic origin of the polarization we examine the average displacements, δ , of the cations within each structure. In the case of the pure BZT and 50% BZT structures we observe that on average all cations preferentially off-center along the c axis of the unit cell, giving rise to the predominantly $[001]$ polarization (Fig. 1). The in-plane components of the off-centering of the 50%–50% alloy are inline with the observed 14° tilt of the polarization away from $[001]$. Indeed, this is also evident in the average tilt angle (θ) of the cation displacements away from $[001]$ (Table I). Furthermore, the standard deviation of the displacements in the x - y plane (up to 0.16 Å for the Bi ions in BZT and up to 0.23 Å for Bi in the 50% BZT–50% BSZN compound) highlights the fact that the cations all displace in a cone around the overall direction of the polarization. This was previously observed in first-principles simulations of BZT (25°) (Ref. 10) and PZT up to (5°),^{18,19} and was explained as a competition between the ions aligning with the overall polarization and repulsion between the A -cations and the bigger of the two B -cations (in this case Zn). This type of displacement competition motif proved to be fundamental in defining the composition-dependent phase diagram of PZT.²⁰

Conversely, for the pure BSZN and the 25% BZT–75% BSZN we observe nearly equal off-center displacements of each cation in the x , y , and z directions. The sole exception is that of the Ti cation displacements, which exhibit a preference toward the $[101]$ direction. Despite this we find very little difference in the magnitude and direction of the total polarization of the two compositions. This implies that the small concentration of Ti does not significantly influence the structure of the material.

Table I lists the average cation off-center displacements (δ) and Born effective charges (Z^*) for the various BZT–BSZN alloys studied. Our results indicate that in all compounds the Bi cations off-center by the greatest amount. Similarly, the enhanced Z^* s of Nb and Ti indicate that these cations should contribute significantly to the total polarization. Interestingly enough, we note substantial displacements of the bigger Zn cation in BZT-rich compounds (i.e., BZT $\geq 50\%$), while in BZT-poor compounds these ions have nominal displacements. These trends were also noted for the relatively large Zr cations in the PZT solid solution.^{18,19}

In PZT, and more recently in BZT, it was shown that the bigger Zr/Zn cations occupied octahedral cages with expanded volumes. When tetragonally distorted they can accommodate larger ionic displacements toward an apical oxygen.^{10,18,19} On the other hand, off-centering in the $[111]$

TABLE I. Structural properties of the BZT-BSZN compositions studied. a and c/a are the lattice parameters. P is the magnitude of the polarization and δ , θ , and Z^* are the average cation off-centering (Å), angle from $[001]$ ($^\circ$) and Born effective charges, respectively.

BZT (%)	Element			Bi			Sr			Zn			Ti			Nb		
	a (Å)	c/a	P ($\mu\text{C}/\text{cm}^2$)	δ	θ	Z^*												
100	3.74	1.22	142	0.89	6	4.4	0.70	1	2.5	0.48	17	4.5
50	3.84	1.11	114	0.67	15	4.3	0.37	23	2.7	0.48	7	2.7	0.35	18	4.5	0.20	22	5.7
25	3.95	1.01	81	0.60	50	4.4	0.32	55	2.6	0.27	51	2.8	0.28	43	4.9	0.26	57	5.8
0	3.95	1.01	77	0.58	55	4.4	0.31	56	2.6	0.25	52	2.8	0.25	51	5.8

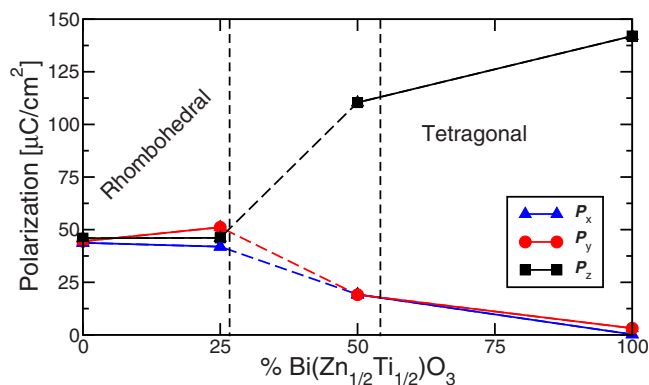


FIG. 2. (Color online) x triangles, y (circles), and z (squares) components of the polarization as a function of BZT concentration. The left of the graph represents structures with polarizations aligned along the [111] (rhombohedral) direction, while to the right we find structures with the polarization mostly oriented along [001].

direction results in displacements toward the face of the octahedral cage. A simple bond-valence argument demonstrated that this causes much stronger repulsions with O ions, thus limiting the overall magnitude of the displacements.²¹ Similar local structure motifs are most likely the origin of the discrepancy in Zn displacements in the BZT–BSZN compounds found here.

Figure 2 depicts the x -, y -, and z -components of the polarization as a function of BZT composition. Here we see that for small concentrations of BZT the polarization is equal in all directions, i.e., pointing along [111]. This produces a rhombohedral phase. On the other hand, concentrations greater than 50% BZT result in a rotation of the polarization to mostly along the [100] direction. Given these results we generate a rough picture of the phase diagram of the BZT–BSZN alloy, which, similar to ferroelectric alloys such as PZT, may exhibit a sharp MPB in the region near 50% BZT.^{2,3}

In summary, we have examined the polarization as a function of composition for alloys of BZT and BSZN. For the structures studied, our results demonstrate that for compositions of $\geq 50\%$ BZT the polarization points mostly along [001]. However, for concentrations with $\leq 25\%$ BZT the polarization is aligned along the [111] direction. Our phase diagram proposes the existence of a monoclinic phase at roughly 50% BZT concentrations. In addition, our structural analysis yields comparable displacement patterns to those observed in DFT calculations on the PZT solid solution, hinting at the possibility of high piezoelectric responses in these materials. Also, the lower polarization in the monoclinic

phase near the cross-over region suggests that these materials will in fact be switchable and thus useful for ferroelectric/piezoelectric applications.

This work was supported by the Materials Sciences and Engineering Division, Office of Basic Energy Sciences, U.S. Department of Energy (V.R.C., D.J.S.), the Office of Naval Research (S.T., D.J.S.) and UNCF (A.H.). This research used resources of the National Energy Research Scientific Computing Center, supported by the Office of Science, U.S. Department of Energy under Contract No. DEAC02-05CH11231.

- ¹H. Fu and R. E. Cohen, *Nature (London)* **403**, 281 (2000).
- ²B. Noheda, D. E. Cox, G. Shirane, J. A. Gonzalo, L. E. Cross, and S.-E. Park, *Appl. Phys. Lett.* **74**, 2059 (1999).
- ³R. Guo, L. E. Cross, S.-E. Park, B. Noheda, D. E. Cox, and G. Shirane, *Phys. Rev. Lett.* **84**, 5423 (2000).
- ⁴S.-E. Park and T. R. Shrout, *J. Appl. Phys.* **82**, 1804 (1997).
- ⁵J. B. Neaton, C. Ederer, U. V. Waghmare, N. A. Spaldin, and K. M. Rabe, *Phys. Rev. B* **71**, 014113 (2005).
- ⁶S. Takagi, A. Subedi, D. J. Singh, and V. R. Cooper, *Phys. Rev. B* **81**, 134106 (2010).
- ⁷R. J. Zeches, M. D. Rossell, J. X. Zhang, A. J. Hatt, Q. He, C.-H. Yang, A. Kumar, C. H. Wang, A. Melville, C. Adamo, G. Sheng, Y.-H. Chu, J. F. Ihlefeld, R. Erni, C. Ederer, V. Gopalan, L. Q. Chen, D. G. Schlom, N. A. Spaldin, L. W. Martin, and R. Ramesh, *Science* **326**, 977 (2009).
- ⁸M. R. Suchomel and P. K. Davies, *Appl. Phys. Lett.* **86**, 262905 (2005).
- ⁹M. R. Suchomel, A. M. Fogg, M. Allix, H. Niu, J. B. Claridge, and M. J. Rosseinsky, *Chem. Mater.* **18**, 4987 (2006).
- ¹⁰T. Qi, I. Grinberg, and A. M. Rappe, *Phys. Rev. B* **79**, 094114 (2009).
- ¹¹D. Vanderbilt, *Phys. Rev. B* **41**, 7892 (1990).
- ¹²P. Giannozzi, S. Baroni, N. Bonini, M. Calandra, R. Car, C. Cavazzoni, D. Ceresoli, G. L. Chiarotti, M. Cococcioni, I. Dabo, A. D. Corso, S. de Gironcoli, S. Fabris, G. Fratesi, R. Gebauer, U. Gerstmann, C. Gougousis, A. Kokalj, M. Lazzeri, L. Martin-Samos, N. Marzari, F. Mauri, R. Mazzarello, S. Paolini, A. Pasquarello, L. Paulatto, C. Sbraccia, S. Scandolo, G. Sclauzero, A. P. Seitsonen, A. Smogunov, P. Umari, and R. M. Wentzcovitch, *J. Phys.: Condens. Matter* **21**, 395502 (2009).
- ¹³H. B. Krause and D. L. Gibbon, *Z. Kristallogr.* **134**, 44 (1971).
- ¹⁴P. K. Davies and M. A. Akbas, *J. Phys. Chem. Solids* **61**, 159 (2000).
- ¹⁵S. A. Prosandeev, E. Cockayne, B. P. Burton, S. Kamba, J. Petzelt, Y. Yuzyuk, R. S. Katiyar, and S. B. Vakhruhev, *Phys. Rev. B* **70**, 134110 (2004).
- ¹⁶See supplementary material at <http://dx.doi.org/10.1063/1.3570626> for detailed figures of the 50% BZT-50% BSZN and the 25% BZT-75% BSZN cation orderings.
- ¹⁷R. D. King-Smith and D. Vanderbilt, *Phys. Rev. B* **47**, 1651 (1993).
- ¹⁸V. R. Cooper, I. Grinberg, N. R. Martin, and A. M. Rappe, *AIP Conf. Proc.* **626**, 26 (2002).
- ¹⁹I. Grinberg, V. R. Cooper, and A. M. Rappe, *Phys. Rev. B* **69**, 144118 (2004).
- ²⁰I. Grinberg, V. R. Cooper, and A. M. Rappe, *Nature (London)* **419**, 909 (2002).
- ²¹V. R. Cooper, I. Grinberg, and A. M. Rappe, *AIP Conf. Proc.* **677**, 220 (2003).